Anton S. Petrov*
Gene Lamm
George R. Pack
Department of Chemistry, University of Louisville, Louisville, KY 40292

Calculation of the Binding Free Energy for Magnesium–RNA Interactions

Received 30 July 2004; accepted 23 September 2004
Published online 4 January 2005 in Wiley InterScience (www.interscience.wiley.com). DOI 10.1002/bip.20171

Abstract: *The nature of the interaction between nucleic acids and divalent ions in solution is complex. It includes long-range electrostatic and short-range nonelectrostatic forces. Water molecules can be in an inner coordination shell that intervenes between the ion and its binding site. This work describes a method for calculating the binding free energy and applies it to a specific Mg–RNA system (Protein Data Bank ID: 1H2R) in the presence of monovalent salt. The approach combines high-level ab initio theory with Poisson–Boltzmann calculations and provides an accurate description of all terms of the binding free energy for magnesium ions located at the RNA surface (including nonelectrostatic interactions). Some alternative macroscopic approaches are also discussed.*
 Biopolymers 77: 137–154, 2005

Keywords: *RNA folding; Mg-nucleic acids; Mg-induced structure; RNA conformation; RNA structure*

INTRODUCTION

The function of RNA molecules in biological systems is closely related to their folded structure.[1,2] During the folding process, the strong electrostatic repulsion between different domains arising from the sugar–phosphate RNA backbone must be overcome. To form a stable folded structure, these unfavorable interactions are partially neutralized by the presence of mono- and/or polyvalent metal cations.[3] While various experimental data indicate that the presence of magnesium ions is not absolutely necessary for the folding of tRNA,[4–7] polyvalent ions, particularly magnesium, are thought to play an important role in determining the functional conformations of many RNAs. For example, the addition of micromolar concentrations of magnesium has been shown to significantly stabilize an RNA pseudoknot,[8] and other data have confirmed that magnesium ions bind specifically to other RNA systems.[9,10] Also, structural studies indicate that Mg^{2+} ions are intimately associated with the tertiary structure of the *Tetrahymena* group I intron,[11,12] which cannot be folded solely in the presence of monovalent salt and does not show catalytic activity in the presence of other divalent metals.[13]

The importance of magnesium in the structural and functional role of RNA systems highlights the need to understand the nature of the interaction. Association constants for magnesium–nucleic acid binding can be determined by methods based on the colligative properties of solutions (such as the osmotic pressure),[14]

Correspondence to: George R. Pack; email: george.pack@louisville.edu
**Present address:* Department of Biology, Georgia Institute of Technology, Atlanta, GA 30332
Biopolymers, Vol. 77, 137–154 (2005)

Scatchard plot analysis,[15,16] NMR,[8,17] electron spin polarization resonance (ESPR)[18] fluorescence titration,[19] and calorimetry.[20] The data are reviewed by Misra and Draper.[21] Generally, the experimental results indicate that the interaction energies for magnesium ions bound to RNA secondary structures (hairpins) are small and depend on the concentration of monovalent salt in the system. However, those ions bound to the tertiary structure have higher affinities that are difficult to measure because of the coupling between ion binding and RNA folding.[22]

Several theories have been proposed to explain the stabilizing role of magnesium ions. Manning's counterion condensation theory[23] provides the most general explanation of the interaction between polyelectrolyte molecules and ions in solution. Additional information about the interaction of magnesium with nucleic acids has also be obtained from Monte Carlo[24,25] and molecular dynamic[26–28] simulations. However, these methods, which are based on empirical potentials, do not treat magnesium ions at a level detailed enough for accurate affinity calculations.[29] High-level electronic structure theory has also been used to obtain the preferential modes for metal binding to nucleic acid fragments. While these calculations primarily apply to the gas phase,[30–33] results relevant to polar media have recently appeared.[34,35]

Many theoretical approaches treat the ions around RNA molecules within the framework of the nonlinear Poisson–Boltzmann (PB) equation.[24,36–40] Most of these models consider a single RNA conformation, although a method that couples magnesium binding to RNA folding has recently been proposed.[41,42] Several attempts to calculate the electrostatic potential of RNA molecules[43] and total binding free energy of metal cations to RNA systems using the PB theory have also appeared.[40,44] Although these studies illustrate how most of the contributions to the binding energy of RNA–metal complexes in ionic solution could be evaluated, their predictions do not agree well with experimental data. The main reason for this lack of agreement is that these computational models assume that the interaction between metal cations and RNA is primarily electrostatic. High-level theoretical calculations of magnesium:nucleic acid–fragment complexes illustrate that the interaction between these species includes significant nonelectrostatic contributions.[29,35] We therefore present a computational method that accounts for both electrostatic and nonelectrostatic contributions to the binding free energy of Mg^{2+}–RNA systems.

THEORY AND METHODS

A Concept of Magnesium RNA–Binding

Polyvalent cations (magnesium, cobalt, spermine, etc.) that neutralize RNA in solution can be divided into two groups.[21] The first group includes diffuse ions that surround RNA. The interaction of these ions with RNA is purely electrostatic and can be reasonably well described by PB theory.[24,39,40] The effect of these cations depends on both relative and absolute concentrations of mono- and divalent cations. At low relative concentrations ($10^{-6}/10^{-3}$ *M*/*M*), divalent cations do not show any significant effect on the binding of monovalent ions.[41] On the other hand, at higher relative concentrations ($10^{-3}/10^{-3}$ *M*/*M*), divalent cations compete with monovalent cations, displacing a significant fraction of them away from the RNA surface. We assume that diffuse ions are separated by at least two layers of water (one layer belongs to the hydration shell of the cation and the other to that of RNA) from the actual nucleic acid surface.[21] These ions are mobile at the RNA surface and exchange with other diffuse cations located near the surface.

The second group of RNA-bound polyvalent counterions is comprised of ions that are bound to specific sites at the nucleic acid surface. Site-bound ions have restricted mobility due to strong attractive interactions that are greater than the thermal energy of the ion. Analysis of crystal structures and theoretical calculations show that the most common binding sites at the nucleic acid surface are the O6 and N7 atoms of guanine bases and anionic oxygen of phosphate groups.[12,45] Although it is questionable whether all observed locations of metal cations in the crystal structures are specific binding sites in solution, theoretical calculations show that the interactions with guanine and phosphate moieties are stronger than interactions with other sites at the nucleic acid surface (see the data in Table I and findings of our group[35,46]). We consider these sites to be primary binding sites that persist even in unfolded RNA. When secondary structure forms, an actual binding site may be comprised of several primary sites as well as other interactions with adjacent bases and even strand crosslinking. It has been proposed[1] that some metal ion binding sites are formed during RNA folding at a higher structural level, that is, when its tertiary structure appears. Such sites may have a more complex structure, and include interactions not only with phosphates and guanines and adjacent bases but also with other bases and sugar moieties. Structurally, metal cations located in such binding sites may crosslink not only two complimentary strands but also two distant regions of RNA.

In general, site-bound ions interact with binding sites either through a single layer of water molecules (outer-sphere coordination) or by forming direct contacts (inner-sphere coordination). The interaction of these ions with RNA can be partitioned into two terms. The first term describes the interaction with the electric field of the negatively charged RNA molecule (which is similar to that observed for diffuse ions) and is purely electrostatic in nature. Second, bound ions are additionally stabilized by

Table I Gas-Phase Electronic Energies (in Hartrees) and Interaction Energies (in kcal/mol) Obtained for m15 and m21 Complexes in Gas Phase at the RHF/6-31+G(d) Level[a]

	Binding Site	$Mg(H_2O)_6^{2+}$	Complex	Interaction Energy
		m15 complex		
E(G112p)	−719.5349881	−655.390811	−1375.148585	−139.8
E(A113p)	−719.5356059	−655.3918336	−1375.216723	−181.5
E(C128p)	−719.5390197	−655.3917828	−1375.163838	−146.2
E(U202p)	−719.5355054	−655.3913556	−1375.167041	−150.7
E(C203p)	−719.5382025	−655.3920055	−1375.22625	−185.8
E_{sum}	−3597.683322	−3276.957789	−6875.922437	−804.0
E_{total}	−3596.902067	−655.3898724	−4253.4673667	−737.6
E_{total}, CP	−3596.910095	−655.3983677	−4253.4673667	−727.2
		m21 complex		
E(U144)	−451.5094975	−655.42214	−1106.973909	−26.5
E(U156)	−451.5087725	−655.42187	−1106.947878	−10.8
E(U157)	−451.5087133	−655.42248	−1106.972208	−25.7
E(G158)	−578.4371106	−655.42227	−1233.931565	−45.3
E_{sum}	−1932.964094	−2621.68871	−4554.825560	−108.5
E_{total}	−1932.949446	−655.4212472	−2588.527532	−98.4
E_{total}, CP	−1932.950939	−655.4251525	−2588.527532	−95.0

[a] *E*(base) is the energy of monomers in binary base–Mg complexes; E_{sum} is the sum of the energies *E*(base); E_{total} is the energy of monomers in m15 and m21 complexes; E_{total}; CP is the counterpoise corrected energy of monomers in m15 and m21 complexes.

specific interactions that are more complex, and include dielectric and salt-screening effects on the Coulombic term and also the quantum effects of charge transfer, atomic polarization, exchange-correlation, and dispersion interactions as well as cavity creation terms, which cannot be described by electrostatics.

Metal cations interact with nucleic acid sites with different relative contributions from the electrostatic and nonelectrostatic terms. Strong short-range nonelectrostatic interactions play a major role in magnesium ion site binding. High-level theoretical gas-phase calculations indicate that the origin of these interactions is primarily due to strong charge transfer and polarization effects.[33,34] Recent studies done within the framework of polarized continuum models combined with density functional theory show that the relative importance of the non-electrostatic interactions becomes even more significant in polar media.[35] Other cations, e.g., K^+, Na^+, and Ca^{2+}, do not show such significant nonelectrostatic interactions as Mg^{2+}. This property of the divalent magnesium ion stems from its small ionic radius (0.86 Å): a high positive charge is localized within a small volume, allowing the ion to approach within 2.05–2.15 Å of atomic nuclei, providing a basis for strong nonelectrostatic interactions. For outer-sphere magnesium– nucleic acid complexes, charge transfer and polarization effects are also significant despite an intervening water molecule. It has been shown that for these complexes charge transfer is water mediated and occurs by a cooperative mechanism.[33] All these facts suggest that in order to properly describe specific interactions of magnesium ions with RNA, both electrostatic and nonelectrostatic interactions must be considered.

Model Description

The nonlinear PB equation can account for the electrostatic interaction of counterions with highly charged polyelectrolyte molecules.[37,47] On the other hand, this method lacks an explicit description of nonelectrostatic interactions, which are known to be very significant in the case of magnesium binding.[21,33,34] Because these interactions can accurately be described by ab initio methods, we suggest a combination of ab initio theory with PB calculations to predict Mg–RNA interaction energies with a high degree of accuracy. This provides a rigorous basis for the calculation of Mg–RNA interactions in the presence of polar media and mobile ions. The thermodynamic cycle approach depicted in Figure 1 splits the calculation of the total free energy associated with Mg–RNA binding into several stages.

Stage 1. Specific binding of magnesium to RNA molecule can be either direct or water mediated through its hydration shell. We consider a binding site (BS) to be comprised of phosphate groups, nucleotide bases, and ribose moieties that have one or both of these contacts with the magnesium ion under consideration. The computational process begins with an all-atom structural model; in the present example we use a crystal stucture.[12] Molecular fragments defining the binding site and the bound, hydrated ion are extracted from the

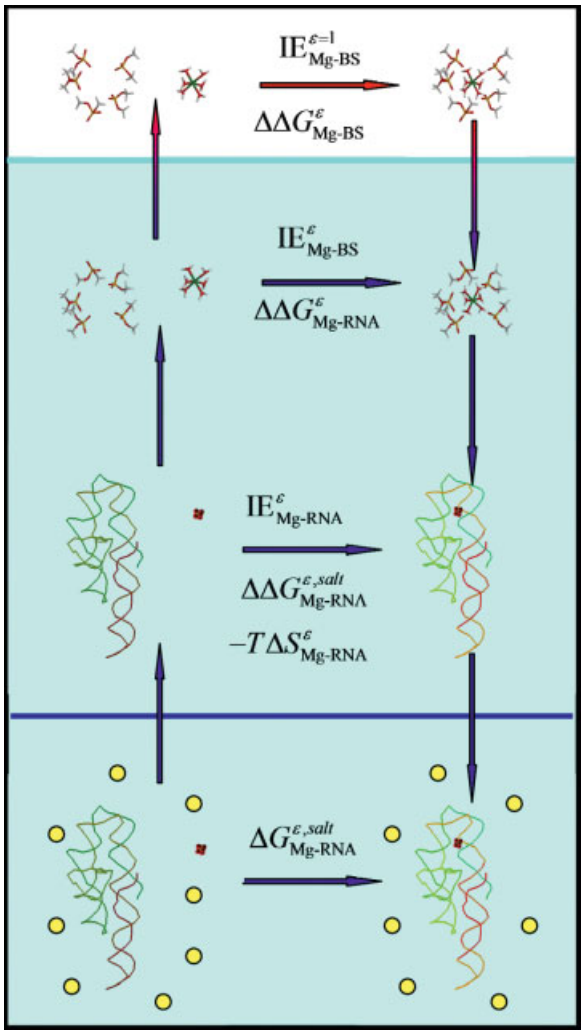

FIGURE 1 The thermodynamic cycle for calculation of the free binding energies in RNA–Mg systems.

RNA structure and capped with hydrogen atoms. The first stage of the thermodynamic cycle is a gas-phase ab initio calculation of the Mg–BS system. Hydrogen atom positions (including those that belong to water molecules of the hydration shell) were found through partial optimization of the corresponding complexes. Heavy atom positions of magnesium ions, bases, and phosphate moieties are taken from the crystal structure and are therefore identical to those in the RNA molecule, as required for the remaining steps of the thermodynamic cycle. Since previous calculations[35] have shown that incorporating environment effects changes the calculated equilibrium geometries of these systems, retention of the crystallographic coordinates for the heavy atoms is not only required for consistency throughout the cycle but is more accurate than using gas-phase-reoptimized geometries. The total interaction energy calculated for this gas-phase system including basis set superposition error (BSSE)[48] is

$$IE^{\epsilon=1}_{\text{Mg–BS}} = E^{\epsilon=1}_{\text{Mg–BS}} - E^{\epsilon=1}_{\text{BS}} - \text{E}^{\epsilon=1}_{\text{Mg}} + \text{BSSE}. \quad (1)$$

Stage 2. The next step is a calculation of the solvation energies of the binding site, the hydrated magnesium ion, and their complex, again with heavy atoms in the experimental geometry and previously optimized hydrogens. There are several methods that may be used to account for the solvent. A simple method treats the system using the generalized Born approach; alternatively, the numerical solution of the Poisson equation can be used. Both of these methods, however, consider only the change in electrostatic properties of the system. To account for solvation effects on all energy changes, including polarization, charge transfer, and other nonelectrostatic components, the Mg–BS system should be treated by polarized continuum models combined with high-level electronic structure theory. The value of the dielectric coefficient at the surface of nucleic acids lies in a range of 30–50.[49] Preliminary calculations, however, have shown that the interaction energy of magnesium–guanine and magnesium–phosphate complexes is almost independent of dielectric coefficient in a range 40–80,[35] allowing us to use the value of 78.4 for the dielectric coefficient in COSMO-polarized continuum model (CPCM) calculations and thus be consistent with other calculations. The total interaction energy between the binding site and the magnesium ion in the presence of polar solvent is calculated as

$$IE^{\epsilon}_{\text{Mg–BS}} = IE^{\epsilon=1}_{\text{Mg–BS}} + \Delta\Delta G^{\epsilon}_{\text{Mg–BS}} + RT\ln(1/22.4), \quad (2)$$

where $\Delta\Delta G^{\epsilon}_{\text{Mg–BS}}$ is the change in the solvation energy of the Mg–BS complex and its monomers, and the last term represents a change in the reference state from gas to water. We note that the aqueous-phase interaction energy could be calculated in a similar manner without recourse to the gas-phase energies, however optimization of hydrogen positions and the BSSE corrections (stage 1) are much more efficiently done in the gas phase.[50,51]

Stage 3. The next step requires the calculation of the interaction energy between magnesium and RNA in a polar solvent but *in the absence of mobile ions*. The basic concept of this step is adapted from the method of Bashford and Karplus[52] and based on the Tanford–Kirkwood approach[53] for the calculation of ionization constants of titratable sites in proteins, which has also been applied to calculate pK_a's for titratable sites in nucleic acids.[54] Protonation of an amino acid in that method is analogous to occupation of a binding site by magnesium in the present approach. The binding site with and without a magnesium ion is dissolved within the full RNA molecule. Binding is associated with a free energy change $\Delta G^{\epsilon}_{\text{Mg–RNA}}$, representing the difference in solvation energy of the binding site with and without the magnesium ion. Solvation energies for this stage can be found by solving the linear Poisson equation and can be thought as the sum of two terms: a Born term representing the energy of moving the binding site from aqueous environment into the RNA dielectric cavity and a term accounting for the interaction with the background charges of RNA. Details of the computational procedure are given in the Methods section. Given the interaction energy between Mg

and its binding site (IE^{ϵ}_{Mg-BS}), the total interaction energy with RNA can be described as

$$IE^{\epsilon}_{Mg-RNA} = IE^{\epsilon}_{Mg-BS} + \Delta\Delta G^{\epsilon}_{Mg-RNA}. \quad (3)$$

To calculate the Mg–RNA free energy of binding in a polar media ($\Delta G^{\epsilon}_{Mg-RNA}$), we should also account for the entropic penalty associated with the displacement of water. Thus, in a polar solvent we have

$$\Delta G^{\epsilon}_{Mg-RNA} = IE^{\epsilon}_{Mg-RNA} - T\Delta S_{Mg-RNA}. \quad (4)$$

Stage 4. The last step in the thermodynamic cycle describes the free energy change upon addition of diffuse electrolyte ions. Since RNA systems are highly charged, the calculation of the free energies of the Mg–RNA complex and its monomers requires the use of the nonlinear PB equation. The standard methodology for this step has been developed and is described elsewhere.[41,47] The alternative Debye–Hückel and generalized Born approximations may also be used to assess this energy term.[44]

In general, both monovalent (sodium, potassium) and divalent (magnesium) ions are present in solution. The screening effect due to magnesium ions, however, is insignificant if their concentration is much smaller than that of monovalent ions.[41] We assume that this is the case for biological systems of interest and consider that the salt is represented by a 1–1 electrolyte with the effect of diffuse magnesium ions neglected for simplicity. According to the proposed thermodynamic cycle, the total standard free energy of magnesium binding to a specific site at the RNA surface in a polar solvent and in the presence of electrolyte is given by

$$\Delta G^{0(\epsilon,\,NaCl)}_{Mg-RNA} = IE^{\epsilon\,=\,1}_{Mg-BS} + \Delta\Delta G^{\epsilon}_{Mg-BS} + \Delta\Delta G^{\epsilon}_{Mg-RNA} + \Delta\Delta G^{\epsilon,\,NaCl}_{Mg-RNA} + RT\ln(1/22.4) - T\Delta S_{Mg-RNA}. \quad (5)$$

Assuming that magnesium site binding can be described by mass action, the total free energy of the magnesium binding can be obtained from a standard Langmuir binding isotherm.[40]

Overall, the proposed method describes the calculation of the free energy of binding of a single magnesium ion to an RNA molecule. This energy is the "intrinsic binding energy" in the terminology of Tanford and Kirkwood since it does not account for interactions with other magnesium ions bound to different sites at the RNA surface. In principle, binding of multiple magnesium ions could be obtained within the framework of the nonlinear PB equation as is done in pK_a calculations.[55]

Computational Details

Gas-Phase Interaction Energy. Binding sites and magnesium ions were extracted from the RNA crystal structure [Protein Data Bank (PDB) ID: 1H2R] and capped with hydrogen atoms. Hydrogen positions were optimized at the restricted Hartree-Fock (RHF)/6-31+G(d) level using the Gaussian 03 suite of programs,[56] while keeping heavy atom positions frozen. Single-point energy calculations were done with the self-consistent field (SCF) = tight option at the same level; the interaction energy was calculated as the difference between single-point energies of the complexes and their monomers. The BSSE was calculated using the counterpoise (CP) correction method of Boys and Bernardi[48] and the deformational energy of complexes and monomers was neglected. Partition of the interaction energy according to Kitaura and Morokuma was performed with the GAMESS package at the RHF/6-31G level using the RHF/6-31 + G(d) optimized geometries and a BSSE correction was applied during the decomposition procedure.

CPCM Calculations. The effect of polar solvent was described within the framework of the CPCM as implemented in the Gaussian 03 package. Solvation energies of the complexes and monomers were calculated using the partially optimized gas-phase structures. The interaction energy in a polar solvent was calculated according to Eq. (2), where the BSSE correction from Stage 1 was included.[50] The molecular cavity was comprised of interlocking spheres centered on solute atoms or atomic groups with radii taken from the United Atom topological model and scaled by a factor of 1.2; calculations were performed with 200 initial tesserae per sphere. The value $\epsilon = 78.4$ was used for the dielectric coefficient of the polar media.

PB Calculations. Both linear and nonlinear PB numerical calculations were performed using finite difference method as implemented in the UHBD program.[62,63] The potential at the boundary of a coarse grid ($75 \times 75 \times 75$) with a grid spacing of 2 Å was calculated by approximating all fixed atoms in the system as Debye–Hückel (DH) spheres. A focusing procedure at the position of the magnesium ion was performed by using a finer grid ($150 \times 150 \times 150$) with a grid spacing of 0.6 Å. The RNA molecule and binding sites were treated as low dielectric media with dielectric coefficient ϵ_{in}. Several values for this dielectric coefficient were used in the range of 1–10. Volumes of the RNA and the binding sites were determined by their solvent-accessible surface area calculated using a probe radius of 1.4 Å. Charges and atomic parameters of RNA were taken from the AMBER ff99 force field,[64] most of which were originally derived from the ff94 force field of Cornell et al.[65]; charges for the binding sites and hexahydrated magnesium ions were derived according to the restrained electrostatic potential (RESP) methodology of Kollman and coworkers.[66]

Geometries of the monomers were taken from the corresponding complexes optimized in the gas phase as discussed earlier with charges calculated at the RHF/6-31G(d) level. The magnesium ion radius used was 0.86 Å.

The solvent was described by an external dielectric coefficient $\epsilon_{out} = 78.4$ (at 300 K). Diffusely bound ions were treated as a 1–1 electrolyte, with a concentration of 0.1 or 0.2*M*. To account for finite ion size, an exclusion distance of

2.0 Å was added at all atoms of RNA, the extracted binding sites and the hexahydrated magnesium ions. Nonlinear contributions of the salt effect were calculated according to a standard methodology as implemented in the UHBD program.[67] For comparison, values of the free energy change due to addition of salt were also calculated using the linearized DH approximation within UHBD.

Generalized Born Calculations. An alternative calculation of interaction energies, solvation energies, and salt contributions to the free energy was performed using the AMBER 7.0 suite of programs[68] with ff99 force field parameters for RNA.[64] Charges for the binding sites and hexahydrated magnesium ions were calculated as described above. Solvent effects were treated within the generalized Born surface area (GBSA) approach[69,70] with the modified set of Bondi radii.[71] The total free energies of species in solution were calculated as the sum of electrostatic (ES), van der Waals (VDW), and solvation (GBSA) contributions. The internal energy of bonds and angles was omitted from consideration since the geometries of all complexes and their monomers were frozen. Salt effects were taken into account by using the DH extension of the generalized Born equations.[72]

Entropy Calculations. The entropic free energy of Mg–RNA binding was calculated by normal mode analysis as implemented in the Nmode module of AMBER 7.0, as suggested by Case et al.[44,73] A dielectric coefficient of $4r_{ij}$ (where r_{ij} represents the distance between the atoms i and j) was used in the calculations. All structures were energy minimized using the Newton–Raphson method until the convergence criterion of 10^{-3} kcal/(mol · Å) for the root mean square of the components of the gradient vector was achieved. Translational and rotational entropic terms were calculated as described by McQuarrie[74] and the vibrational contribution was estimated from calculated normal mode frequencies at 300 K.[75]

Solvation Energy Calculations. The free energy difference $\Delta\Delta G^{\epsilon}_{\mathrm{Mg-RNA}}$ associated with the transfer of the binding site and its hydrated magnesium ion to the RNA molecule was calculated by applying a modified version of the Bashford–Karplus (BK) approach[52] for the calculation of ionization constants of titratable sites in proteins.

The calculation of the free energy difference consisted of two steps. In the first step, the binding site with and without the hexahydrated magnesium ion is transferred to the dielectric cavity of RNA with the atomic charges of RNA set to zero. Application of the BK method requires that the positions of all atoms in the RNA molecule and binding sites be identical in order to allow cancellation of self-energy terms, thus necessitating removal of the capping hydrogen atoms of the binding sites that were used in the calculation of the hydration energy ($\Delta\Delta G^{\epsilon}_{\mathrm{Mg-BS}}$). The energy associated with this part of the solvation process represents the Born contribution to the free energy and can be expressed as[76]

$$\Delta\Delta G_{\mathrm{Born}}(\mu) = \frac{1}{2}\sum_{i\in\mu}^{\mathrm{Mg-BS}} Q_i^{\mathrm{Mg-BS}}[\phi^{\mathrm{Mg}}_{\mathrm{RNA}}(Q_i^{\mathrm{Mg-BS}}|r_i) - \phi^{\mathrm{Mg}}_{\mathrm{BS}}(Q_i^{\mathrm{Mg-BS}}|r_i)] - \frac{1}{2}\sum_{i\in\mu}^{\mathrm{BS}} Q_i^{\mathrm{BS}}[\phi^{0}_{\mathrm{RNA}}(Q_i^{\mathrm{BS}}|r_i) - \phi^{0}_{\mathrm{BS}}(Q_i^{\mathrm{BS}}|r_i)]. \quad (6)$$

The notation $\phi^{\mathrm{Mg}}_{\mathrm{RNA}}(Q_i^{\mathrm{Mg-BS}}|r_i)$ represents the value of the electrostatic potential in RNA (distinct from that in the binding site) at position r_i of the atom i belonging to binding site μ. The superscript 0 for the potential refers to unbound states of RNA and the binding site.

In the second step of this solvation process, the background RNA charges are turned on. The energy associated with doing this represents the additional Coulomb interaction with the background charges. For simplicity, we charge the magnesium ion at the RNA surface in the presence of the electric field of the background atoms instead of charging the RNA background in the presence of the magnesium ion. Thus, we have

$$\Delta\Delta G_{\mathrm{back}}(\mu) = \sum_{i\in\mu}^{\mathrm{Mg-BS}} (Q_i^{\mathrm{Mg}} - Q_i^{0})\phi^{\mathrm{back}}(q^{\mathrm{back}}|r_i|) \quad (7)$$

where r_i represents the potential due to background charges q^{back} calculated at the positions r_i of the removed charges of the binding site and magnesium ion.

The total change in the free energy difference for the process of solvation of the binding site in the RNA molecule with and without magnesium is the sum of terms (6) and (7). We note that the magnesium ion alone does not change its charge state during this process.

RESULTS AND DISCUSSION

System Description

The P4–P6 domain of the *Tetahymena thermophila* group I intron has been a paradigm in the numerous experimental and theoretical studies of cation binding.[17,40,43,44] The ΔC209 mutant of this RNA molecule has been crystallized in the presence of $MgCl_2$ and the crystal structure of this Mg–RNA complex has recently been determined (PDB ID: 1HR2).[12] This RNA molecule cocrystallizes as a dimer with 27 magnesium ions bound to its surface. The structure of the monomeric RNA fragment is shown in Figure 2a.

We classify bound magnesium ions into three groups. The first group contains ions located in the major groove of double-helical fragments and are predominantly bound to the O6 and N7 atoms of guanine. Most of these ions are hexahydrated and form outer-sphere complexes. Representatives of this

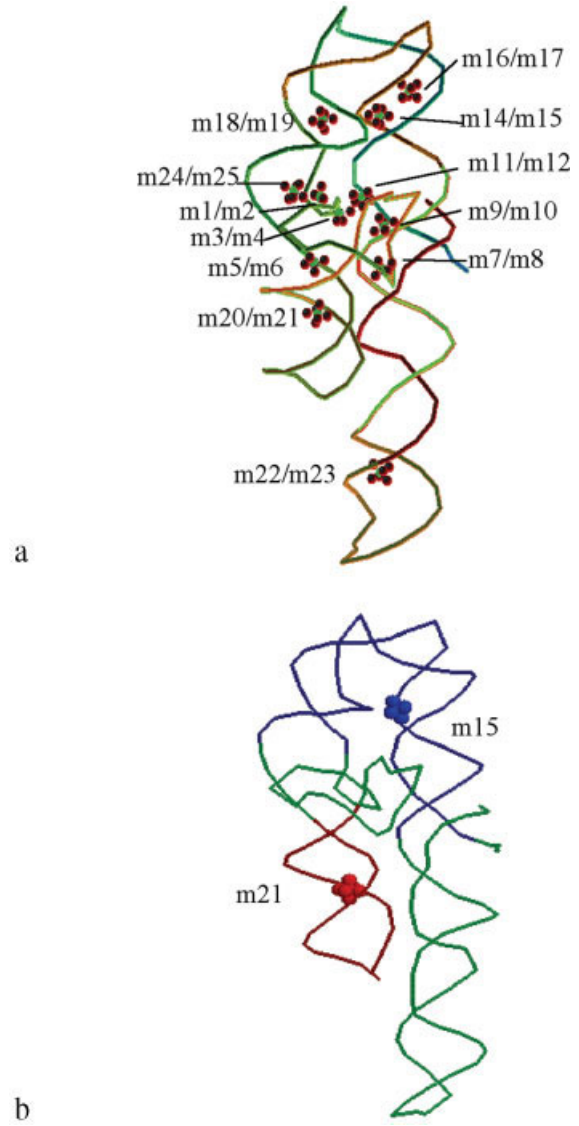

FIGURE 2 Tertiary structure of the P4–P4 domain of the *Tetahymena thermophila* group I intron (a) overlaid with magnesium ions found in the crystal structure (numbers are given for magnesiums of both RNA molecules in the asymmetric unit); (b) colored according to fragments studied here; m15 complex shown in blue and m21 complex shown in red.

group are m5/6, m9/10, m16/17, m18/19, m20/21, m22/23, and m24/25. Magnesium ions of a second type (m1/2, m3/4, and m7/8) are located in A-rich bulges. All of these are partially dehydrated ions and form inner-sphere (direct) contacts with phosphate groups of the nucleotides comprising the bulge. The loss of water molecules from the first coordination sphere is compensated by formation of favorable interactions with phosphates. The third class is represented by m11/12 and m14/15, which crosslink remote domains of the RNA molecule. Although these ions are also bound to phosphate groups, unlike ions in the previous group, most form water-mediated contacts with RNA.

In the current study we consider the interaction between fragments of the P4–P6 *Tetrahymena* group I intron and two hexahydrated magnesium ions, m15 and m21 (Figure 2b). Experimental binding energies are available for the complex containing ion m21.[17] Both of these ions are hexahydrated in the bound state, thus simplifying the calculations. The binding site for m15 contains phosphates of nucleotides G112, A113, C128, U201, and C203, and is represented by five dimethylphosphate anions (DMP^-) (Figure 3a). The P4, P5, and P5a domains, including U107–G134 and C189–A214 nucleotides, were chosen to represent the full RNA molecule for the m15 ion. The m21 binding site is neutral and consists of three uracil

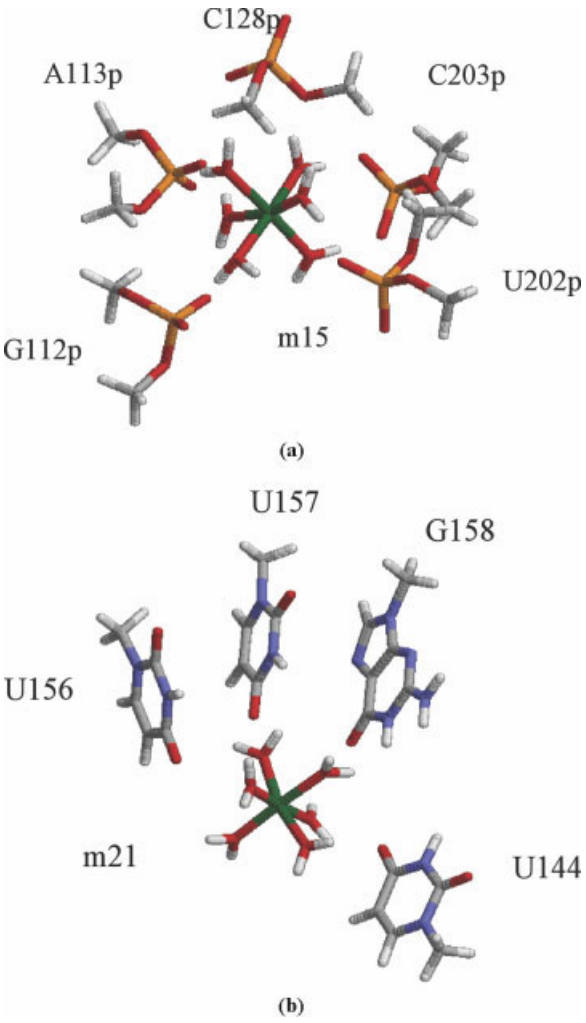

FIGURE 3 Binding site for magnesium ions (a) m15 and (b) m21.

bases (U144, U156, U157) and guanine base G158 (Figure 3b). The P5b hairpin containing A139–G164 nucleotides served as the RNA fragment for m21. These two systems represent magnesium-binding sites at the surface of the RNA molecule that are different chemically as well as structurally.

Gas-Phase Interaction Energies for the m15 and m21 Complexes

The interaction energy for m15 and m21 in the complexes with their binding sites is presented in Table I. Interaction of m15, bound to the negatively charged binding site (charge −5), results in an energy of −727.2 kcal/mol. Each interaction with an individual DMP^- contributes about 130–170 kcal/mol, although the sum of the pairwise interactions overestimates the value of the total energy by 14%, due to nonadditive many-body effects. The interaction energy for m21 is much smaller, reflecting the neutrality of the binding site. Analysis of the pairwise interactions indicates that the main contribution to binding comes from the interaction of m21 with G158. The strength of this interaction is due to the favorable direction of the dipole of guanine with respect to the magnesium ion.[33] The pairwise interactions overestimate the total binding energy by 10.5%. Since the Hartree–Fock level does not account for electron correlation, we also calculated the pairwise interactions at the MP2 level using the same basis set and found no significant change. Extensive density functional theory (DFT) calculations of $Mg^{2+}(H_2O)_6$ with both guanine and dimethylphosphate,[35] combined with the present results, lead us to conclude that the RHF level is sufficient to adequately describe magnesium binding in these systems.

The interaction energies for these complexes, calculated as a sum of Coulombic interactions between point charges, was found to be −744.3 and −64.5 kcal/mol for the m15 and m21 complexes, respectively. Decomposition of the interaction energy into electrostatic (ES), polarization (PL), charge transfer (CT), exchange-correlation (EX), and mixed (MIX) components performed according to the Kitaura–Morokuma scheme[57] indicated that the electrostatic component of the interaction energy is underestimated by the point-charge approximation, especially for the m21 complex (see Table II). Reasons for the failure of this approximation are discussed in detail elsewhere.[35,77] The decomposition data also indicate that the largest relative interactions in the m15 complex are electrostatic, as expected from its high charge. A greater relative contribution from the polarization and charge-transfer terms to the stabilization was found for the m21 complex, although the magnitude of these terms was less than that seen for the m15 complex.

Table II Decomposition of the Interaction Energy for m15 and m21 Complexes performed by Kitara–Morokuma Scheme at the RHF/6-31G level with BSSE[a]

	m15	m21
ES	−765.2	−82.0
EX	63.0	12.2
POL	−36.3	−24.7
CT	−22.1	−8.3
MIX	8.5	1.7
IE	−752.0	−101.0

[a] Values of the electrostatic (ES), exchange-correlation (EX), polarization (POL), charge transfer (CT), and mixing (MIX) components of the interaction energy (IE) are shown.

Interaction Energies for m15 and m21 Complexes in a Polar Medium

Both the m15 and m21 complexes are significantly destabilized in the presence of polar media ($\epsilon = 78.4$). Solvation and binding energy data are presented in Table III. These values were calculated within the framework of the CPCM model and also by solving the Poisson equation (i.e., the PB equation in the absence of electrolyte). The general trend for the solvation energies of the species can be understood in terms of simple Born theory: they are proportional to the squared charge of the system and inversely proportional to the radius. Solvation energies calculated by CPCM differ from the Poisson-calculated energies because the CPCM method accounts for nonelectrostatic effects. In particular, the Poisson method includes neither the energy of cavity formation nor the dispersion and repulsion terms. For the complex formed by m15, $\Delta\Delta G^{\epsilon}_{Mg-BS}$ calculated by the CPCM and PB methods at the same geometry are 651.6 and 707.2 kcal/mol; the corresponding values for m21 are 82.8 and 67.4 kcal/mol. The change in the surface area of the complexes and monomers, calculated in the CPCM method but not in the Poisson approach, accounts for most of the energy difference.

Table III also contains binding energies (IE^{ϵ}_{Mg-BS}). calculated using the Poisson equation. for the complexes of m15 and m21. The energy for m15 (−38.1 kcal/mol) is much more negative than that obtained by a simple scaling of the electrostatic interactions (−744.3 kcal/mol) by the reciprocal dielectric coefficient (1/78.4). This is because m15 is located inside a low-dielectric

Table III Electronic (in Hartrees) and Solvation and Interaction (in kcal/mol) Energies Calculated for the m15 and m21 Binding Site Complexes[a]

	Binding Site	$Mg(H_2O)_6^{2+}$	Complex	Interaction Energy
		m15		
$E_{HF,CP}$	−3596.91009	−655.39836	−4253.46736	−727.2
$\Delta G^{\epsilon}_{Mg-BS}$ (CPCM)	−698.3	−178.0	−224.8	651.6
E^{ϵ}_{Mg-BS} (CPCM-CP)	−3598.01491	−655.67355	−4253.82556	−87.9 (−77.5)
E_{elec}				−744.3
$\Delta G^{\epsilon}_{Mg-BS}$ (PB)	−871.9	−212.3	−377.0	707.2
E^{ϵ}_{Mg-BS} (PB)				−38.1
		m21		
$E_{HF,CP}$	−1932.95094	−655.42515	−2588.52753	−95.0
$\Delta G^{\epsilon}_{Mg-BS}$ (CPCM)	−9.3	−169.3	−95.6	82.8
E^{ϵ}_{Mg-BS} (CPCM-CP)	−1932.96423	−655.69104	−2588.67853	−16.5 (−13.1)
E_{elec}				−64.5
$\Delta G^{\epsilon}_{Mg-BS}$ (PB)	−86.4	−204.4	−223.4	67.4
E^{ϵ}_{Mg-BS} (PB)				2.9

[a] $E_{HF,CP}$: single-point energy calculated at the HF/6-31+G(d) level with counterpoise correction; $\Delta G^{\epsilon}_{Mg-BS}$ (CPCM): solvation energy calculated by the CPCM model; E^{ϵ}_{Mg-BS} (CPCM-CP): energy in a polar solvent calculated by the CPCM model (with counterpoise correction); E_{elec}: Coulombic electrostatic energy; $\Delta G^{\epsilon}_{Mg-BS}$ (PB): solvation energy calculated by the PB equation; E^{ϵ}_{Mg-BS} (PB): energy in a polar solvent calculated by the PB equation.

cavity formed by five DMP^- groups, all of which are immersed in a high-dielectric medium. The slightly positive binding energy found for m21 (2.9 kcal/mol) could be due to several factors. First of all, the geometry of this complex was optimized in vacuo, not in the electrostatic field described by the Poisson equation. Second, electrostatic interactions calculated based on the atom-centered RESP charges are underestimated at the surfaces of monomers.[77]

The total interaction energies obtained by the CPCM method corrected for the gas-phase BSSE and the change in the reference state[50] are −77.5 and −13.1 kcal/mol for the m15 and m21 complexes, respectively. These energies account not only for the electrostatic interactions between species but also include the nonelectrostatic effects of polarization and charge transfer, as well as a change in surface area of the cavity in the polar medium.[78] Direct comparison of the data obtained by the CPCM and Poisson methods indicates that inclusion of these nonelectrostatic terms significantly stabilizes the complexes. This is particularly important because these energy terms enter into Eq. (5) without cancellation.

Transfer of the m15 and m21 Binding Sites into RNA

Stage 3 in the thermodynamic cycle is the transfer of the binding site (with and without magnesium) into the environment of RNA. For each BS and Mg–BS system, this transfer can be thought as a two-step process. In the first (Born) stage, a solute interacts with the uncharged RNA cavity; the second (back) stage accounts for the stabilization of the solute by background RNA charges. The differences in ΔG^{ϵ} between the BS and Mg–BS systems for these stages of the thermodynamic cycle are given by Eqs. (6) and (7), respectively.

Table IV presents the values of these energy terms calculated for the m15 and m21 complexes for different values of the internal dielectric coefficient of RNA. For the m15 complex, the Born energy term is −6.2 kcal/mol when $\epsilon_{in} = 1$ and decreases to −4.4 kcal/mol as ϵ_{in} is increased to 4. These data indicate that a low dielectric cavity (surrounding the complex) stabilizes the Mg–BS interaction for m15—a higher dielectric coefficient serves to screen the interaction. The stabilization is reversed for the m21 complex. The Born energy difference for this system was found to be 11.1 and 3.3 kcal/mol for the values of $\epsilon_{in} = 1$ and 4, respectively. These calculations yield positive values for the Born energy term, indicating that the interaction between the binding site and the ion is destabilized by the low dielectric RNA cavity. The large difference in the Born energies for these two sites is due to the relative positioning of the Mg-binding sites within the cavities. The low dielectric RNA cavity completely surrounds the magne-

Table IV Born, Background, and Total Solvation Free Energy Differences (in kcal/mol) Calculated for m15 and m21 Complexes[a]

	m15 (1)	m15 (4)	m21 (1)	m21 (4)
$\Delta\Delta G_{\text{Born}}$	−6.2	−4.4	11.1	3.3
$\Delta\Delta G_{\text{back}}$	−35.6	−33.2	−25.6	−25.9
$\Delta\Delta G^{\epsilon}_{\text{RNA–Mg}}$	−41.8	−37.6	−14.4	−22.7

[a] Calculations performed with the values of the internal dielectric coefficient given in parentheses.

sium-binding site complex for m15, thus enhancing the interaction. However, m21 is located at the surface of RNA so that in this case RNA acts as a low dielectric boundary, destabilizing the binding interaction. An analytical demonstration of this phenomenon for systems of spherical symmetry (a sphere in the field of the external point charge) can be found in Böttcher's monograph.[79]

In addition to the Born energy, transferring the binding complex to an RNA environment involves an interaction with the background charges of the RNA molecule. The data in Table IV show that these interactions are almost independent of the dielectric coefficient of the cavity. Changing this parameter from 1 to 4 decreases the interaction from −35.6 kcal/mol to −33.2 kcal/mol for m15 and increases the strength of this interaction from −25.6 kcal/mol to −26.0 kcal/mol for m21. These data illustrate the degree to which the presence of the negative background charges stabilizes the Mg ion for both binding sites. This stabilization is stronger for m15 because the double-helical fragment of RNA containing domains P4, P5, and P5a is bent, leading to a larger background electrostatic potential at the magnesium ion position than that for m21, for which the RNA conformation is linear.

Overall, the effect of the RNA is to stabilize the interaction of m15 and m21 with the binding site, as indicated by the negative values of $\Delta\Delta G^{\text{Mg–RNA}}_{\epsilon}$ given in Table IV; the stabilization is significantly larger for m15 than for m21. For m15, the net stabilization at $\epsilon_{\text{in}} = 1$ (−41.8 kcal/mol) is greater than that for $\epsilon_{\text{in}} = 4$ (−37.6 kcal/mol), whereas this trend is reversed (−14.4 and −22.7 kcal/mol, respectively) for m21. This dielectric coefficient dependence correlates with the Born energy difference.

Entropic Contributions

The entropic contribution to the free energy of Mg–RNA binding can be estimated by normal mode analysis as implemented in AMBER. This procedure requires energy minimization of the structures of the Mg–RNA complexes. The minimization procedure failed when applied to the RNA fragment that binds m15 and we present the calculation of the entropic term only for the m21 complex.

The translational, rotational, and vibrational contributions to the total binding entropy are presented in Table V, although the relevance of the rotational component is questionable. By measuring the EPR spectra of $Mn(H_2O)_6^{2+}$, it has been shown that the rotational correlation time of the cation increases when bound to the ribosome, indicating a change in rotational motion.[80] On the other hand, NMR data has shown that for the analogous binding of $Co(NH_3)_6^{3+}$, all 18 amino protons are equivalent on the microsecond timescale despite no observed rotation of the cation over the course of a 3-ns molecular dynamics simulation.[44] We include the rotational entropic contribution in our calculations because the rotation for $Mg(H_2O)_6^{2+}$ in the bound and unbound states should more resemble that of $Mn(H_2O)_6^{2+}$. Overall, we found that the translational and rotational contributions destabilize Mg–RNA interactions by 12.1 and 8.7 kcal/mol, respectively.

It has been pointed out that the calculation of the vibrational contribution may also be problematic. Tsui and Case have shown that values for this term calculated using different minimized structures (cor-

Table V Entropic Contributions of m21 Complex from Normal Mode Analysis (Values Represent $-TS$ (in kcal/mol) Calculated at 300 K)

	RNA	$Mg(H_2O)_6^{2+}$	Complex	Interaction Energy
Translational	−15.9	−12.1	−15.9	12.1
Rotational	−16.1	−8.6	−16.0	8.7
Vibrational	−707.0	−15.0	−733.1	−11.1
Total	−738.9	−35.8	−764.9	9.8

responding to different local energy minima) may vary by a few kcal/mol.[44] We performed minimization of the crystal structure and found that the vibrational term increases the binding free energy by 11.1 kcal/mol at 300 K. The total entropic contribution destabilizes the binding free energy of the m21 complex by 9.8 kcal/mol. We use this value as an estimate for the entropy term of the m15 complex as well, recognizing the limitations as discussed above.

The Effect of Diffuse Ions Around RNA

The effect of added salt was calculated based on the nonlinear PB equation with $\epsilon_{in} = 1$ and assuming an ionic strength of 0.1*M* (assuming a 1:1 electrolyte). This led to a decrease in the binding free energy by 36.1 and 19.5 kcal/mol for the m15 and m21 complexes, respectively, due to screening of the dominant electrostatic contribution (refer to Tables II and VI). Setting $\epsilon_{in} = 4$ did not significantly alter the salt contributions. An increase in salt concentration to 0.2*M* produced only insignificant additional destabilization. These data show that at high salt concentration the fraction of diffuse ions at the surface is almost independent of the ionic strength, as predicted by Manning's counterion condensation theory[23] and by related Monte Carlo and PB calculations.[24]

The destabilization energies estimated by solving the linearized version of the PB equation (the DH approximation) are significantly smaller than those predicted by the full PB equation. The solution for 0.1 (0.2) *M* salt ($\epsilon_{in} = 1$) shows a destabilization of only 22.6 (26.5) and 12.2 (15.1) kcal/mol for the m15 and m21 complexes, respectively. The main reason for this is that the potential at the surface of RNA calculated using the DH approximation is severely overestimated.[81] The salt concentration dependence calculated within the DH approximation is quite significant compared with that obtained by solving the PB equation, consistent with ascribing the phenomenon of counterion condensation to the nonlinear form of the latter.[76]

The Standard Free Energy of Binding

The total standard free energy of interaction between RNA and a single magnesium ion in a polar solvent and in the presence of diffuse ions is given by Eq. (5). It consists of terms describing (1) the interaction between the binding site and a magnesium ion in the gas phase, (2) the correction for the presence of the polar solvent, (3) a term that accounts for the transfer of the binding site into the RNA cavity, (4) the entropic penalty of binding, and (5) the contribution of added salt. This energy is an "intrinsic binding energy" calculated in the absence of other specifically bound ions and, therefore, does not account for the mutual interaction of other bound ions. However, this effect is not expected to be large due to the effects of electrolyte screening.

The free energy of binding calculated for complexes m15 and m21 are summarized in Table VI. Since an all-atom representation of RNA was used and polarization and charge transfer effects were treated explicitly, we compare results obtained with $\epsilon_{in} = 1$ with the experimental data. For the thermodynamic cycle shown in Figure 1, these free energies are −72.4 and 2.7 kcal/mol for the m15 and m21 complexes, respectively. Such a large difference in binding energies is explained by the position of the binding site in the RNA molecule. Ion m15 interacts with five negatively phosphate groups of RNA and is located in a low-dielectric binding pocket fully enclosed by the negatively charged molecule. Ion m21, on the other hand, interacts with a neutral binding site located at the macromolecular surface. The calculated binding energy for the m21 complex, although positive (2.7 kcal/mol), is not far from the determination by Tinoco et al.,[17] who measured the binding affinities for the P5b Mg–RNA complex in the presence of 0.2*M* NaCl and found that the binding free energy for this system is −3.5 kcal/mol. Although the experimental measure is not directly comparable to our calculated values—it represents binding of all (diffuse and site-bound) Mg—in view of the paucity of experimental data on these interactions we note the result.

The results of calculations performed with $\epsilon_{in} = 4$ are also presented in Table VI. These energies were −69.5 and −7.2 kcal/mol for the m15 and m21, respectively. Compared to the calculated values of the energy found with $\epsilon_{in} = 1$ (−72.4 and 2.7 kcal/mol), the free energy slightly decreased for complex m15 and increased for m21. Examination of the contributions to the total binding free energy (Tables IV and VI) shows that most of the terms in Eq. (5) are essentially independent of the value of the internal dielectric coefficient, the exception being the interaction with the RNA cavity ($\Delta\Delta G_{Born}$). The dependence of this term on the dielectric coefficient is qualitatively identical to that observed for the total free energy. Therefore, the interaction of magnesium with the RNA cavity determines the dielectric coefficient dependence of the binding free energy.

Alternative Methods

The free energy of Mg–RNA interactions can also be evaluated by several classical schemes that do not

Table VI Energies of m15 and m21 RNA Complexes (in kcal/mol) Calculated Using the Thermodynamic Cycle[a]

	m15 (1)	m15 (4)	m21 (1)	m21 (4)
$\Delta E_{\mathrm{HF,CP}}$	−727.2	−727.2	−95.0	−95.0
$IE^{\epsilon}_{\mathrm{Mg-BS}}$	−77.5	−77.5	−13.1	−13.1
$\Delta\Delta G^{\epsilon}_{\mathrm{Mg-RNA}}$	−41.8	−37.6	−14.4	−22.7
$\mathrm{IE}^{\epsilon}_{\mathrm{Mg-RNA}}$	−119.3	−115.1	−27.5	−35.8
$-T\Delta S_{\mathrm{Mg-RNA}}$	9.8	9.8	9.8	9.8
$\Delta\Delta G^{\epsilon,\,salt}_{\mathrm{Mg-RNA}}$ (DH, 0.1)	22.6	22.1	12.2	11.7
$\Delta\Delta G^{\epsilon,\,salt}_{\mathrm{Mg-RNA}}$ (PB, 0.1)	36.1	34.8	19.5	17.8
$\Delta\Delta G^{\epsilon,\,salt}_{\mathrm{Mg-RNA}}$ (DH, 0.2)	26.5	25.9	15.1	14.3
$\Delta\Delta G^{\epsilon,\,salt}_{\mathrm{Mg-RNA}}$ (PB, 0.2)	37.0	35.8	20.4	18.8
$\Delta G^{\epsilon,\,salt}_{\mathrm{Mg-RNA}}$ (PB, 0.2)	−72.4	−69.5	2.7	−7.2

[a] See footnotes for Table III $\Delta\Delta G^{\epsilon}_{\mathrm{Mg-RNA}}$: PB solvation energy difference at zero salt; $\mathrm{IE}^{\epsilon}_{\mathrm{Mg-RNA}}$: interaction energy in a polar solvent at zero salt ($\mathrm{IE}^{\epsilon}_{\mathrm{BS-Mg}} + \Delta\Delta G^{\epsilon}_{\mathrm{RNA-Mg}}$); $-T\Delta S_{\mathrm{Mg-RNA}}$: entropic penalty; $\Delta\Delta G^{\epsilon,\,salt}_{\mathrm{Mg-RNA}}$ (DH, 0.1): 0.1*M* salt contribution obtained by solving the DH equation; $\Delta\Delta G^{\epsilon,\,salt}_{\mathrm{Mg-RNA}}$ (PB, 0.1): 0.1*M* salt contribution obtained by solving the PB equation $\Delta\Delta G^{\epsilon,\,salt}_{\mathrm{Mg-RNA}}$ (DH, 0.2): 0.2*M* salt contribution obtained by solving the DH equation; $\Delta\Delta G^{\epsilon,\,salt}_{\mathrm{Mg-RNA}}$ (PB, 0.2): 0.2*M* salt contribution obtained by solving the PB equation; $\Delta G^{\epsilon,\,salt}_{\mathrm{Mg-RNA}}$ (PB, 0.2): total free energy [$\mathrm{IE}^{\epsilon}_{\mathrm{Mg-RNA}} - T\Delta S_{\mathrm{Mg\text{-}RNA}} + \Delta\Delta G^{\epsilon,\,salt}_{\mathrm{RNA-Mg}}$ (PB, 0.2)]. Calculations performed with the values of the internal dielectric coefficient given in parentheses.

account for quantum effects. A detailed description of these schemes is given elsewhere.[44] To demonstrate the necessity of including the nonelectrostatic components in the calculation of the binding free energies, we present the results of alternative calculations performed for the same systems using empirical potentials from AMBER.

According to the scheme suggested by Tsui and Case,[44] solvation energies are calculated as the sum of gas-phase interactions, solvation terms, entropic contributions, and the effect of added salt. The principal difference between this and our scheme is in the calculation of the gas-phase term, which could be estimated, for instance, within the AMBER ff99 force field. Since this interaction could be calculated between a magnesium ion and the entire RNA molecule, no extraction of the binding site would be necessary. The solvation terms can be estimated either by solving the Poisson equation or by applying the generalized Born surface area model. Similar methods can also account for the presence of salt.

Tables VII and VIII present calculations of the binding energies for the m15 and m21 complexes using the classical ff99 potentials and the Poisson equation. We found that the interactions between RNA and the corresponding magnesium ions in polar solvent are −76.5 (−54.3) and −4.3 (−23.2) kcal/mol if $\epsilon_{\mathrm{in}} = 1$ (4) was used. By comparing these numbers with those calculated using the quantum chemical methods described in previous sections (Table VI), we see that the classical calculations result in significantly smaller binding energies for both systems. The effect of salt for these systems as calculated from the linear and nonlinear PB equations has been described previously (see section, The Effect of Diffuse Ions Around DNA, above). The total free energy of Mg–RNA binding obtained by PB calculations in the presence of 0.2*M* of salt in polar solvent with $\epsilon_{\mathrm{in}} = 1$ (4) was found to be −29.7 (−8.7) and 25.9 (5.4) kcal/mol, respectively. In both cases the interactions are weaker than those obtained using the thermodynamic cycle because of the neglect of nonelectrostatic components.

PB calculations combined with the data of the empirical ff99 force field on Mg–RNA systems also reveal that a dependence of the binding energy on ϵ_{in} is similar to that obtained using the thermodynamic cycle shown in Figure 1. An increase in ϵ_{in} from 1 to 4 leads to destabilization of the enclosed m15 system, whereas the surface-bound m21 system becomes more stable. The reason for this difference is the same as previously discussed and due to different effects of the RNA cavity. Noting that for complex m21 an increase in ϵ_{in} leads to stabilization of the interaction, we also performed calculations of the binding free energy for this complex using $\epsilon_{\mathrm{in}} = 10$. As anticipated, additional stabilization of the complex was observed and the total binding energy in the presence

Table VII Energies of m15 RNA Complex (in kcal/mol) Calculated Using the PB Equation Combined with the f99 Force Field[a]

	RNA	$Mg(H_2O)_6^{2+}$	Complex	Interaction Energy
		$\epsilon_{in} = 1$		
E_{elec}	27093.6	−211.1	24014.3	−2868.2
E_{VDW}	17.2	31.9	47.3	−1.9
E_{gas}	27110.8	−179.2	24061.6	−2870.1
$\Delta G^{\epsilon}_{Mg-RNA}$	−35664.1	−212.3	−33082.9	2793.6
E^{ϵ}_{Mg-RNA}	−8553.3	−391.5	−9021.3	−76.5
$-TS_{Mg-RNA}$	−738.9	−35.8	−764.9	9.8
$\Delta G^{\epsilon,\,salt}_{Mg-RNA}$ (DH, 0.2)	−330.9	−0.7	−305.1	26.5
$\Delta G^{\epsilon,\,salt}_{Mg-RNA}$ (PB, 0.2)	−402.4	−0.7	−366.1	37.0
$G^{\epsilon,\,salt}_{Mg-RNA}$ (PB, 0.2)	−9694.6	−428.0	−10152.3	−29.7
		$\epsilon_{in} = 4$		
E_{elec}	6773.4	−52.8	6003.6	−717.0
E_{VDW}	17.3	31.9	47.2	−1.9
E_{gas}	6790.7	−20.9	6050.8	−718.9
$\Delta G^{\epsilon}_{Mg-RNA}$	−8502.3	−50.8	−7888.6	664.6
E^{ϵ}_{Mg-RNA}	−1711.6	−71.7	−1837.8	−54.3
$-TS_{Mg-RNA}$	−738.9	−35.8	−764.9	9.8
$\Delta G^{\epsilon,\,salt}_{Mg-RNA}$ (DH, 0.2)	−324.6	−0.7	−299.4	25.9
$\Delta G^{\epsilon,\,salt}_{Mg-RNA}$ (PB, 0.2)	−389.2	−0.7	−354.1	35.8
$G^{\epsilon,\,salt}_{Mg-RNA}$ (PB, 0.2)	−2839.7	−108.2	−2956.8	−8.7

[a] E_{elec}: Coulombic electrostatic energy; E_{VDW}: van der Waals energy, E_{gas}: total gas energy; $\Delta G^{\epsilon}_{Mg-RNA}$: PB solvation energy at zero salt; E^{ϵ}_{Mg-RNA}: energy in a polar solvent at zero salt ($E_{gas} + \Delta G^{\epsilon}_{Mg-RNA}$); $-TS_{Mg-RNA}$: entropic penalty; $\Delta G^{\epsilon,\,salt}_{Mg-RNA}$ (DH, 0.2): 0.2*M* salt contribution obtained by solving the DH equation; $\Delta G^{\epsilon,\,salt}_{Mg-RNA}$ (PB, 0.2): 0.2*M* salt contribution obtained by solving the PB equation; $\Delta G^{\epsilon,\,salt}_{Mg-RNA}$ (PB, 0.2): total free energy [$E^{\epsilon}_{Mg-RNA} - TS_{Mg-RNA} + \Delta G^{\epsilon,\,salt}_{Mg-RNA}$ (PB, 0.2)].

of 0.2*M* salt was found to be 3.3 kcal/mol, which is not far from the experimental value. The use of a high internal dielectric coefficient is not appropriate for the m15 complex because the Mg ion is buried inside the RNA molecule.

As an alternative to the PB method, we also performed calculations of the free energy of binding using the ff99 force field and treating the solvent within the generalized Born model. The results of these calculations for the m15 and m21 complexes are presented in Tables XI and X, respectively. The solvation energy terms were found to be −69.0 (−45.8) and −6.6 (−18.4) kcal/mol for the calculations performed with $\epsilon_{in} = 1$ (4) and agree with the corresponding energy terms obtained by solving the PB equation as given in Tables VI and VIII (especially those using $\epsilon_{in} = 1$). The penalties due to the presence of 0.2*M* monovalent salt in these systems found by combining the GB potential with a DH screening term are 36.2 and 15.6 kcal/mol. The salt effect calculated by this method for the m21 system agrees with that obtained by solving the linear PB equation, whereas comparison for m15 shows that this term was overestimated. However, it coincidentally agrees with that calculated by solving the nonlinear PB equation. In general, the binding free energies calculated by the generalized Born method are consistent with those obtained by the PB method with both methods underestimating the Mg–RNA interaction.

DISCUSSION

Magnesium ions bound to specific locations at the RNA surface interact with the polyelectrolyte in a complex way, including specific electrostatic and nonelectrostatic interactions with the binding site, long-range electrostatic attraction by RNA backbone, solvent and salt effects, and entropic penalties. Whereas the PB equation is an excellent tool to describe solvent and salt effects on the electrostatic interactions, it lacks nonelectrostatic

Table VIII Energies of m21 RNA Complex (in kcal/mol) Calculated Using the PB Equation Combined with the f99 Force Field[a]

	RNA	$Mg(H_2O)_6^{2+}$	Complex	Interaction Energy
		$\epsilon_{in} = 1$		
E_{elec}	5418.9	−230.1	3666.7	−1522.0
E_{VDW}	−276.3	31.1	−247.9	−2.7
E_{gas}	5142.6	−199.0	3418.8	−1524.7
$\Delta G^{\epsilon}_{Mg-RNA}$	−9407.6	−201.3	−8088.4	1520.4
E^{ϵ}_{Mg-RNA}	−4265.0	−400.3	−4669.6	−4.3
$-TS_{Mg-RNA}$	−738.9	−35.8	−764.9	9.8
$\Delta G^{\epsilon,\,salt}_{Mg-RNA}$ (DH, 0.2)	−75.9	−0.7	−61.4	15.2
$\Delta G^{\epsilon,\,salt}_{Mg-RNA}$ (PB, 0.2)	−95.9	−0.7	−76.2	20.4
$G^{\epsilon,\,salt}_{Mg-RNA}$ (PB, 0.2)	−5099.8	−436.8	−5510.7	25.9
		$\epsilon_{in} = 4$		
E_{elec}	1354.7	−57.5	916.7	−380.5
E_{VDW}	−276.3	31.1	−247.9	−2.7
E_{gas}	1078.4	−26.4	668.8	−383.2
$\Delta G^{\epsilon}_{Mg-RNA}$	−2236.3	−48.3	−1924.6	360.0
E^{ϵ}_{Mg-RNA}	−1157.9	−74.7	−1255.8	−23.2
$-TS_{Mg-RNA}$	−738.9	−35.8	−764.9	9.8
$\Delta G^{\epsilon,\,salt}_{Mg-RNA}$ (DH, 0.2)	−73.8	−0.7	−60.2	14.3
$\Delta G^{\epsilon,\,salt}_{Mg-RNA}$ (PB, 0.2)	−91.4	−0.7	−73.3	18.8
$G^{\epsilon,\,salt}_{Mg-RNA}$ (PB, 0.2)	−1988.2	−111.2	−2094.0	5.4
		$\epsilon_{in} = 10$		
E_{elec}	541.9	−23.0	366.7	−152.2
E_{VDW}	−276.3	31.1	−247.9	−2.7
E_{gas}	265.6	8.1	118.8	−154.9
$\Delta G^{\epsilon}_{Mg-RNA}$	−809.2	−17.7	−697.2	129.7
E^{ϵ}_{Mg-RNA}	−543.6	−9.6	−578.4	−25.1
$-TS_{Mg-RNA}$	−738.9	−35.8	−764.9	9.8
$\Delta G^{\epsilon,\,salt}_{Mg-RNA}$ (DH, 0.2)	−71.3	−0.7	−58.6	13.4
$\Delta G^{\epsilon,\,salt}_{Mg-RNA}$ (PB, 0.2)	−85.6	−0.7	−67.664	18.7
$G^{\epsilon,\,salt}_{Mg-RNA}$ (PB, 0.2)	−1368.2	−46.1	−1411.0	3.3

[a] See footnotes for Table VII.

contributions that are important for magnesium–nucleic acid binding. Here we have proposed a scheme that is capable of treating these nonelectrostatic contributions. The complexity of this scheme requires us to discuss the possible sources of error that may occur.

In the proposed method, we used the geometries of the complexes and monomers extracted from the crystal structure (or NMR data). The extracted binding sites were capped with hydrogen atoms whose positions were optimized in a gas-phase calculation. Previous findings on simple systems indicate that gas-phase optimization leads to an underestimation of the binding energy in a polar solvent by a few kcal/mol.[35] This can be avoided by optimization within the CPCM model. Another approximation of these calculations is neglect of the deformational energy of monomers upon binding or their relaxation upon dissociation (that is, extraction). In our case, the geometry was taken from the crystal structure, which is assumed to have the minimum energy structure for the complex in solution (though not necessarily at electrolyte strengths different from the experimental value). Relaxation of monomers necessarily decreases the calculated binding energy. Tsui and Case showed that neglect of the deformational effect is insignificant when the metal–RNA system is treated by the classi-

Table IX Energies of m15 RNA Complex (in kcal/mol) Calculated Using the Generalized Born Equation Combined with the f99 Force Field[a]

	RNA	$Mg(H_2O)_6^{2+}$	Complex	Interaction Energy
		$\epsilon_{in} = 1$		
E_{elec}	27093.6	−211.1	24014.3	−2868.2
E_{VDW}	17.3	31.9	47.3	−1.9
E_{gas}	27110.9	−179.2	24061.6	−2870.1
$\Delta G^{\epsilon}_{Mg-RNA}$	−35152.8	−222.9	−32574.6	2801.1
E^{ϵ}_{Mg-RNA}	−8041.9	−402.1	−8513.0	−69.0
$-TS_{Mg-RNA}$	−738.9	−35.8	−764.9	9.8
$\Delta G^{\epsilon,\,salt}_{Mg-RNA}$ (GB, 0.1)	−453.0	−2.8	−419.7	36.1
$\Delta G^{\epsilon,\,salt}_{Mg-RNA}$ (GB, 0.2)	−454.0	−2.8	−420.7	36.2
$G^{\epsilon,\,salt}_{Mg-RNA}$ (GB, 0.2)	−9234.8	−440.7	−9698.6	−23.0
		$\epsilon_{in} = 4$		
E_{elec}	6773.4	−52.8	6003.6	−717.0
E_{VDW}	17.3	31.9	47.3	−1.9
E_{gas}	6790.7	−20.8	6050.8	−718.0
$\Delta G^{\epsilon}_{Mg-RNA}$	−8447.5	−53.6	−7827.9	673.1
E^{ϵ}_{Mg-RNA}	−1656.8	−74.4	−1777.1	−45.8
$-TS_{Mg-RNA}$	−738.9	−35.8	−764.9	9.8
$\Delta G^{\epsilon,\,salt}_{Mg-RNA}$ (GB, 0.1)	−453.0	−2.8	−419.7	36.1
$\Delta G^{\epsilon,\,salt}_{Mg-RNA}$ (GB, 0.2)	−454.0	−2.8	−420.7	36.2
$G^{\epsilon,\,salt}_{Mg-RNA}$ (GB, 0.2)	−2849.7	−113.0	−2962.7	0.1

[a] See footnotes for Table VII. $\Delta G^{\epsilon,\,salt}_{Mg-RNA}$ (GB, 0.1): 0.1*M* salt contribution obtained by solving the generalized Born equation; $\Delta G^{\epsilon,\,salt}_{Mg-RNA}$ (GB, 0.2): 0.2*M* salt contribution obtained by solving the generalized Born equation; $G^{\epsilon,\,salt}_{Mg-RNA}$ (GB, 0.2): total free energy [$E^{\epsilon}_{Mg-RNA} - TS_{Mg-RNA} + \Delta G^{\epsilon,\,salt}_{Mg-RNA}$ (GB, 0.2)].

cal PB approach.[44] Overall, the approximations discussed above create errors of opposite sign that tend to cancel each other.

It is essential to choose an optimal value for the internal dielectric coefficient in the calculation of the energy of transfer of the binding site into the RNA cavity. Correct consideration of the effect of added salt is also critical in determining the binding energy. Because polarization of the binding site by magnesium was explicitly considered in our approach, we assumed that the use of $\epsilon_{in} = 1$ was appropriate within the framework of the proposed thermodynamic cycle. The meaning of this parameter has been highlighted often in recent literature with a particularly cogent discussion given by Schutz and Warshel.[82] They argue that, in the calculations of the pK_a in proteins, the internal dielectric coefficient is a parameter whose numerical value depends on the complexity of the model used in calculations.

According to Schutz and Warshel, the PB scheme used in the calculations of the binding free energy for Mg–RNA systems represents a macroscopic model that does not accurately treat interactions on the microlevel. In fact, a high value of the internal dielectric coefficient ($\epsilon_{in} = 20$) is often suggested for pK_a calculations.[83] Although such a large value does not have any direct physical implication, it appears to compensate for missing terms in the calculation of ionization (binding) energies and gives good agreement with experimental data.

Since both polarization and charge transfer lead to additional stabilization of cation–nucleic acid system, they can be mimicked by increasing the value of the dielectric coefficient, a result that strongly affects the solvation energy terms. Therefore, we also used a high value (10) for ϵ_{in} for the m21 system within the PB method. The free energy of binding was found to be 3.3 kcal/mol, reasonably close to the experimental data and suggesting that an even higher value for ϵ_{in} might be used. However, this method will fail for the binding of m15, which was found to be less stable if one uses a high dielectric coefficient. As discussed above, the difference in these systems is explained by the location of the ions. High values of the dielectric coefficient may also lead to poor results for the ionization constants of titratable sites buried inside the dielectric cavity of proteins.[84,85] Therefore, low values of the ϵ_{in} should be used in the calcu-

Table X Energies of m21 RNA Complex (in kcal/mol) Calculated Using the Generalized Born Equation Combined with the f99 Force Field[a]

	RNA	$Mg(H_2O)_6^{2+}$	Complex	Interaction Energy
		$\epsilon_{in} = 1$		
E_{elec}	5418.9	−230.2	3666.7	−1522.0
E_{VDW}	−276.3	31.145	−247.9	−2.7
E_{gas}	5142.6	−199.0	3418.8	−1524.7
$\Delta G^{\epsilon}_{Mg-RNA}$	−9170.7	−211.7	−7864.3	1518.1
E^{ϵ}_{Mg-RNA}	−3660.1	−408.6	−4075.4	−6.6
$-TS_{Mg-RNA}$	−738.9	−35.8	−764.9	9.8
$\Delta G^{\epsilon,\,salt}_{Mg-RNA}$ (GB, 0.1)	−117.9	−2.625	−105.0	15.5
$\Delta G^{\epsilon,\,salt}_{Mg-RNA}$ (GB, 0.2)	−118.4	−2.702	−105.5	15.6
$G^{\epsilon,\,salt}_{Mg-RNA}$ (GB, 0.2)	−4517.4	−447.1	−4945.8	18.8
		$\epsilon_{in} = 4$		
E_{elec}	1354.7	−57.5	916.7	−380.5
E_{VDW}	−276.3	31.1	−247.9	−2.7
E_{gas}	1078.4	−26.4	668.8	−383.2
$\Delta G^{\epsilon}_{Mg-RNA}$	−2203.8	−50.9	−1889.9	364.8
E^{ϵ}_{Mg-RNA}	860.9	−75.3	767.4	−18.4
$-TS_{Mg-RNA}$	−738.9	−35.8	−764.9	9.8
$\Delta G^{\epsilon,\,salt}_{Mg-RNA}$ (GB, 0.1)	−117.9	−2.6	−105.0	15.5
$\Delta G^{\epsilon,\,salt}_{Mg-RNA}$ (GB, 0.2)	−118.4	−2.7	−105.5	15.6
$G^{\epsilon,\,salt}_{Mg-RNA}$ (GB, 0.2)	3.6	−113.7	−103.0	7.0

[a] See footnotes for Table IX.

lations of the binding energies for the buried binding sites.

Consideration of the dielectric coefficient as an empirical parameter provides a basis for generalized Born models and macroscopic PB calculation of cation binding energies at sites located at the RNA surface. However, in general, the amount of nonelectrostatic contributions and other components that are not considered at the macroscopic level varies for different binding sites and metal cations. Therefore, although an accurate calculation of the binding energy within the macroscopic models is possible, the optimal choice of the internal dielectric coefficient is not known a priori.

The suggestion of treating bulky magnesium ions by solving the PB equation subject to an artificially low temperature effectively increases the electrostatic potential seen by the ions.[86] Hence, a low-temperature PB approach can be used as an alternative to invoking a high internal dielectric coefficient when calculating the binding free energy for cation–RNA systems, although some basis for an a posteriori temperature choice is required as well.

CONCLUSIONS

We have presented the calculation of the binding free energies between two fragments of ΔC209 mutant of the P4–P6 domain of the *Tetahymena thermophila* group I intron and two magnesium ions (m15 and m21). It has been shown that these specifically bound ions exhibit complex interactions with the polyelectrolyte. Besides electrostatic interactions, the extent of nonelectrostatic contributions has been revealed. The presence of electrolyte and entropic effects influence the total binding energy as well.

We found two ways to describe the interactions in such systems. One way is to calculate terms explicitly using a thermodynamic cycle and treating the system at the microscopic level. The results of these calculations for complex m21 were in a reasonable agreement with experimental data. As an alternative, simple approaches based on the macroscopic PB or generalized Born method may also be used. However, the choice of internal dielectric coefficient is very important in these calculations. Hence, we demonstrated that the consistent prediction of binding energies can

be made using models with different levels of complexity. This suggests that our approach might lead to a greater understanding of the complex interactions between RNA and ionic species and ultimately illuminate the important problem of RNA folding.

The authors would like to thank Prof. Andrew N. Lane for helpful discussions.

REFERENCES

1. Tinoco, I., Jr.; Bustamante, C. J Mol Biol 1999, 293, 271.
2. Silverman, K. S.; Zheng, M. X.; Wu, M.; Tinoco, I.; Cech, T. R. RNA—A Publication of the RNA Society 1999, 5, 1665.
3. Anderson, C. F.; Record, M. T. ARPC 1995, 46, 657.
4. Bolton, P. H.; Kearns, D. R. Biochemistry 1977, 16, 5729.
5. Bolton, P. H.; Kearns, D. R. Biochem Biophys Acta 1977, 477, 10.
6. Cole, P. E.; Crothers, D. M.; Yang, S. K. Biochemistry 1972, 11, 4358.
7. Reid, B. R.; Robillard, G. T. Nature 1975, 257, 287.
8. Gonzalez, R. L.; Tinoco, I. J Mol Biol 1999, 289, 1267.
9. Bassi, G. S.; Murchie, A. I. H.; Lilley, D. M. J. RNA—A Publication of the RNA Society 1996, 2, 756.
10. Stein, A.; Crothers, D. M. Biochemistry 1976, 15, 160.
11. Cate, J. H.; Gooding, A. R.; Podell, E.; Zhou, K.; Golden, B. L.; Kundrot, C. E.; Cech, T. R.; Doudna, J. A. Science 1996, 273, 1678.
12. Juneau, K.; Podell, E.; Harrington, D. J.; Cech, T. R. Structure 2001, 9, 221.
13. Celander, D. W.; Cech, T. R. Science 1991, 251, 401.
14. Anderson, C. F.; Record, M. T. ARPC 1982, 33, 191.
15. Sander, C.; Tso, P. O. P. J Mol Biol 1971, 55, 1.
16. Archer, B. G.; Craney, C. L.; Krakauer, H. Biopolymers 1972, 11, 781.
17. Colmenarejo, G.; Tinoco, I. J Mol Biol 1999, 290, 119.
18. Danchin, A.; Gueron, M. Eur J Biochem 1970, 16, 532.
19. Romer, R.; Hach, R. Eur J Biochem 1975, 55, 271.
20. Rialdi, G.; Biltonen, R.; Levy, J. Biochemistry 1972, 11, 2472.
21. Misra, V. K.; Draper, D. E. Nucleic Acid Sci 1998, 48, 113.
22. Misra, V. K.; Draper, D. E. J Mol Biol 2002, 317, 507.
23. Manning, G. S. J Phys Chem B 1969, 51, 924.
24. Pack, G. R.; Wong, L.; Lamm, G. Biopolymers 1999, 49, 575.
25. Korolev, N.; Lyubartsev, A. P.; Nordenskiold, L. J Biomol Struct Dyn 2002, 20, 275.
26. Reblova, K.; Spackova, N.; Sponer, J. E.; Koca, J.; Sponer, J. Nucleic Acids Res 2003, 31, 6942.
27. Auffinger, P.; Bielecki, L.; Westhof, E. Chem Biol 2003, 10, 551.
28. Auffinger, P.; Bielecki, L.; Westhof, E. J Mol Biol 2004, 335, 555.
29. Gresh, N.; Sponer, J. E.; Spackova, N.; Leszczynski, J.; Sponer, J. J Phys Chem B 2003, 107, 8669.
30. Sponer, J.; Sabat, M.; Burda, J. V.; Leszczynski, J.; Hobza, P.; Lippert, B. J Biol Inorg Chem 1999, 4, 537.
31. Sponer, J.; Leszczynski, J.; Hobza, P. Biopolymers 2001, 61, 3.
32. Sponer, J.; Burda, J. V.; Leszczynski, J.; Hobza, P. J Biomol Struct Dyn 1999, 17, 61.
33. Petrov, A. S.; Lamm, G.; Pack, G. R. J Phys Chem B 2002, 106, 3294.
34. Rulisek, L.; Sponer, J. J Phys Chem B 2003, 107, 1913.
35. Petrov, A. S.; Pack, G. R.; Lamm, G. J Phys Chem B 2004, 108, 6072.
36. Sharp, K. A.; Friedman, R. A.; Misra, V.; Hecht, J.; Honig, B. Biopolymers 1995, 36, 245.
37. Sharp, K. A.; Honig, B. Curr Opin Struct Biol 1995, 5, 323.
38. Sharp, K. A. Biopolymers 1995, 36, 227.
39. Draper, D. E.; Misra, V. K.; Conn, G. C. Abstracts of Papers of the American Chemical Society 2000, 220, U193–U194.
40. Misra, V. K.; Draper, D. E. Proc Natl Acad Sci USA 2001, 98, 12456.
41. Misra, V. K.; Draper, D. E. J Mol Biol 1999, 294, 1135.
42. Misra, V. K.; Shiman, R.; Draper, D. E. Biopolymers 2003, 69, 118.
43. Chin, K.; Sharp, K. A.; Honig, B.; Pyle, A. M. Nature Struct Biol 1999, 6, 1055.
44. Tsui, V.; Case, D. A. J Phys Chem B 2001, 105, 11314.
45. Munoz, J.; Sponer, J.; Hobza, P.; Orozco, M.; Luque, F. J. J Phys Chem B 2001, 105, 6051.
46. Magnuson, E. C.; Koehler, J.; Lamm, G.; Pack, G. R. Int J Quantum Chem 2002, 88, 236.
47. Sharp, K. A.; Honig, B. J Phys Chem B 1990, 94, 7684.
48. Boys, S. F.; Bernardi, F. Mol Phys 1970, 19, 553.
49. Lamm, G.; Pack, G. R. J Phys Chem B 1997, 101, 959.
50. Aquino, A. J. A.; Tunega, D.; Haberhauer, G.; Gerzabek, M. H.; Lischka, H. J Phys Chem A 2002, 106, 1862.
51. Cammi, R.; Delvalle, F. J. O.; Tomasi, J. Chem Phys 1988, 122, 63.
52. Bashford, D.; Karplus, M. Biochemistry 1990, 29, 10219.
53. Tanford, C.; Kirkwood, J. G. J Am Chem Soc 1957, 79, 5333.
54. Pack, G. R.; Wong, L.; Lamm, G. Inter J Quantum Chem 1998, 70, 1177.
55. Bashford, D.; Karplus, M. J Phys Chem 1991, 95, 9556.
56. Frisch, M. J.; Trucks, G. W.; Schlegel, H. B.; Scuseria, G. E.; Robb, M. A.; Cheeseman, J. R.; Montgomery, J. A.; Vreven, T.; Kudin, K. N.; Burant, J. C.; Millam, J. M.; Iyengar, S. S.; Tomasi, J.; Barone, V.; Mennucci, B.; Cossi, M.; Scalmani, G.; Rega, N.; Petersson, G. A.; Nakatsuji, H.; Hada, M.; Ehara, M.; Toyota, K.; Fukuda, R.; Hasegawa, J.; Ishida, M.; Nakajima, T.; Honda, Y.; Kitao, O.; Nakai, H.; Klene, M.; Li, X.; Knox, J. E.; Hratchian, H. P.; Cross, J. B.; Adamo, C.; Jaramillo, J.; Comperts, R.; Stratmann, R. E.; Yazyev,

O.; Austin, A. J.; Cammi, R.; Pomelli, C.; Ochterski, J.; Ayala, P. Y.; Morokuma, K.; Voth, A.; Salvador, P.; Dannenberg, J. J.; Zakrzewski, V. G.; Dapprich, S.; Daniels, A. D.; Strain, M. C.; Farkas, O.; Malick, D. K.; Rabuck, A. D.; Raghavachari, K.; Foresman, J. B.; Ortiz, J. V.; Cui, Q.; Baboul, A. J.; Clifford, S.; Cioslowski, J.; Stefanov, B. B.; Liu, G.; Liashenko, A.; Piskorz, P.; Komaromi, I.; Martin, R. L.; Fox, D. J.; Keith, T.; Al-Laham, M. A.; Peng, C. Y.; Nanayakkara, A.; Challacombe, M.; Gill, P. M. W.; Johnson, B.; Chen, W.; Wong, M. W.; Gonzalez, C.; Pople, J. A. Gaussian 03 (Revision B4); Gaussian, Inc.: Pittsburgh PA, 2003.

57. Kitaura, K.; Morokuma, K. Int J Quantum Chem 1976, 10, 325.
58. Schmidt, M. W.; Baldridge, K. K.; Boatz, J. A.; Elbert, S. T.; Gordon, M. S.; Jensen, J. H.; Koseki, S.; Matsunaga, N.; Nguyen, K. A.; Su, S. J.; Windus, T. L.; Dupuis, M.; Montgomery, J. A. J Comp Chem 1993, 14, 1347.
59. Andzelm, J.; Kolmel, C.; Klamt, A. J Chem Phys 1995, 103, 9312.
60. Barone, V.; Cossi, M. J Phys Chem A 1998, 102, 1995.
61. Barone, V.; Cossi, M.; Tomasi, J. J Chem Phys 1997, 107, 3210.
62. Davis, M. E.; Madura, J. D.; Luty, B. A.; Mccammon, J. A. Comput Phys Commun 1991, 62, 187.
63. Madura, J. D.; Briggs, J. M.; Wade, R. C.; Davis, M. E.; Luty, B. A.; Ilin, A.; Antosiewicz, J.; Gilson, M. K.; Bagheri, B.; Scott, L. R.; Mccammon, J. A. Comput Phys Commun 1995, 91, 57.
64. Wang, J. M.; Cieplak, P.; Kollman, P. A. J Comp Chem 2000, 21, 1049.
65. Cornell, W. D.; Cieplak, P.; Bayly, C. I.; Gould, I. R.; Merz, K. M., Jr.; Ferguson, D. M.; Spellmeyer, D. C.; Fox, T.; Caldwell, J. W.; Kollman, P. J Am Chem Soc 1995, 117, 5179.
66. Cornell, W. D.; Cieplak, P.; Bayly, C. I.; Kollman, P. A. J Am Chem Soc 1993, 115, 9620.
67. Micu, A. M.; Bagheri, B.; Ilin, A.; Scott, L. R.; Pettitt, B. M. J Comp Phys 1997, 136, 263.
68. Case, D. A.; Pearlman, D. A.; Cadwell, J. W.; Cheatham, T. E., III.; Wang, J.; Ross, W. S.; Simmerling, C. L.; Darden, T. A.; Merz, K. M.; Stanton, R. V.; Cheng, A. L.; Vincent, J. J.; Crowley, M.; Tsui, V.; Gohkle, H.; Radmer, R. J.; Duan, Y.; Pitera, J.; Massova, I.; Seibel, G. L.; Singh, U. C.; Weiner, P. K.; Kollman, P. A. AMBER; University of California, San Francisco, 2002; Vol 7.
69. Bashford, D.; Case, D. A. ARPC 2000, 51, 129.
70. Tsui, V.; Case, D. A. Biopolymers 2000, 56, 275.
71. Onufriev, A.; Bashford, D.; Case, D. A. J Phys Chem B 2000, 104, 3712.
72. Srinivasan, J.; Trevathan, M. W.; Beroza, P.; Case, D. A. Theor Chim Acta 2002, 101, 426.
73. Case, D. A. In Computer Simulation of Biomolecular Systems: Theoretical and Experimental Applications; van Gunsteren, W. F., Weiner, P. K., Wilkinson, A. J., Eds.; Kluwer/Escom: Dordrecht, 1997; pp 284–301.
74. McQuarrie, D. A. Statistical Mechanics; Harper & Row: New York, 1975.
75. Srinivasan, J.; Cheatham, T. E., III.; Cieplak, P.; Kollman, P.; Case, D. A. J Am Chem Soc 1998, 120, 9403.
76. Lamm, G. In Reviews in Computational Chemistry; Lipkowitz, K. B., Larter, R., Cundari, T. R., Eds.; Wiley & Sons, Inc.: Hoboken, NJ, 2003; pp 147–365.
77. Jensen, F. Introduction to Computational Chemistry; John Wiley: New York, 1999.
78. Contador, J. C.; Aguilar, M. A.; Sanchez, M. L.; Delvalle, F. J. O. Theochem J Mol Struct 1994, 120, 229.
79. Bottcher, C. J. F.; Belle, O. C. Dielectrics in Static Fields; 2d ed. completely rev ed.; Elsevier Scientific Pub. Co: Amsterdam, 1973.
80. Misra, S. K. Appl Magne Reson 1996, 10, 193.
81. Pack, G. R. Int J Quantum Chem 1982, 9, 81.
82. Schutz, C. N.; Warshel, A. Proteins Struct Funct Genet 2001, 44, 400.
83. Antosiewicz, J.; Mccammon, J. A.; Gilson, M. K. J Mol Biol 1994, 238, 415.
84. Demchuk, E.; Wade, R. C. J Phys Chem B 1996, 100, 17373.
85. Warwicker, J. Protein Sci 1999, 8, 418.
86. Lamm, G.; Pack, G. R. Biophys J 2004, 87, 764.

Reviewing Editor: Dr. David A. Case